2025 International Conference On Rehabilitation Robotics (ICORR)
May 12-16, 2025. Chicago, IL, USA

A Novel Template-Matching Method for Extracting Gait Cycles from Underfoot Pressure Data

Grange M. Simpson, Kylee North, Sonny T. Jones, Ashley N. Dalrymple

***Abstract*— The isolation of gait cycles from underfoot pressure data is a critical step in human movement analysis, yet existing methods require either expensive equipment or substantial manual effort. We present a generalizable, low-resource algorithm for parsing gait cycles from wearable underfoot pressure sensor data across multiple walking terrains. Compared to a ground-truth dataset manually marked and verified by an expert, our algorithm achieved similar accuracy with significantly reduced processing time. For a dataset of 577 steps, our algorithm parsed gait cycles in 41 seconds with only one false negative, whereas three naïve manual parsers required an average of 29 minutes, with total errors ranging from 6 to 33 gait cycles. The algorithm also outperformed threshold-based parsing, which produced 49–362 false positives, depending on the threshold value. By improving computational efficiency with accuracy, this method enables scalable gait cycle detection in real-world applications, expanding the feasibility of automated gait analysis beyond controlled laboratory environments.**

***Index Terms*— Gait Analysis, Walking, Underfoot Pressure, Ground Reaction Force, Rehabilitation**

I. Introduction

Advances in gait analysis and rehabilitation technology, such as wireless sensors, motion capture, exoskeletons, and gait assistance devices, have created a growing demand for efficient, high-quality data analysis methods. A critical component of gait analysis is isolating complete individual gait cycles. Historically, gait analysis has relied on motion capture systems in controlled laboratory settings, but the field is rapidly shifting toward wearable sensors that enable data collection in real-world environments [1]–[3]. This shift presents new challenges, particularly the need for generalizable data reduction and analysis techniques to parse individual gait cycles effectively. The ability to automatically parse gait cycles is particularly challenging when gait data are collected in variable walking environments or with populations that have motor impairments [4].

Gait data from wearable underfoot pressure sensors exhibit substantial variability due to changing walking speeds, terrains, and patient footwear in both healthy individuals and those with motor deficits from musculoskeletal or neurological conditions [5], [6]. These factors complicate the development of standardized analysis pipelines to identify key events, such as the transition from swing to stance phase (i.e., heel strike, marked by the onset of loading), which is critical for parsing gait cycles. Existing pipelines to parse gait cycles, including manual labeling, thresholding, and neural networks [7]–[9], are resource-intensive and have notable limitations. Access to gait experts who can dedicate the time necessary to manually mark large datasets is often limited, leaving the task to naïve parsers. Manual labeling is prone to human bias, time-consuming, and difficult to generalize across datasets and applications [10]. Thresholding entails setting a minimum value to indicate the onset of limb loading [9]. It is prone to false positives with variable pressure, shuffling, or bumping of the foot, requiring the use of catch statements to exclude missteps. Neural networks require large pre-labeled training datasets, extensive computational power, and expertise in machine learning [7]. Previous work has applied a template-based approach to angular velocity signals, but the template was made for waveforms across the entire gait cycle, limiting its generalizability [4].

This work introduces a novel template-matching framework forefficient, generalizable, low-resource gait cycle parsing. A semi-automated approach allows users to mark the onset of limb loading in a subset of data via an intuitive graphical user interface (GUI). After the parser marks the onset of loading, a shape template is generated, capturing the characteristic pressure pattern at the transition from the swing to stance phase. This allows the algorithm to identify similar events across the dataset. This template-matching method was compared to standard methods of parsing gait cycles, including manual labeling by experts and naïve researchers, and thresholding. By overcoming the limitations of existing gait cycle parsing methods, this template-matching framework offers a simple yet scalable and transferable solution for isolating gait cycles, which supports the growing needs of locomotor and rehabilitation research and real-world gait applications.

II. Methods

A. Participants and Data Acquisition

Four male participants with no known neuromuscular deficits were recruited for this study after providing written informed consent following the University of Utah Institutional Review Board (IRB00171076). Participants were 31, 19, 27, and 25 years of age (mean weight = 182.25 ± 17.90 lbs).

A wireless pressure insole containing 235 embedded pressure sensors (XSensor High-Resolution Intelligent Insoles Pro, Calgary, AB, Canada) was placed in each shoe and

We thank the Departments of Biomedical Engineering and Physical Medicine and Rehabilitation for funding this study. We also thank our participants for volunteering their time.

G. M. Simpson (corresponding author e-mail grange.simpson @utah.edu), K. North, S.T. Jones are with the Department of Biomedical Engineering, University of Utah, Salt Lake City, UT, USA. A.N. Dalrymple (corresponding email ashley.dalrymple@utah.edu) is with the Departments of Biomedical Engineering and Physical Medicine and Rehabilitation, University of Utah, Salt Lake City, UT, USA.

2025 International Conference On Rehabilitation Robotics (ICORR) | 979-8-3503-8068-2/25/$31.00 ©2025 IEEE | DOI: 10.1109/ICORR66766.2025.11063134

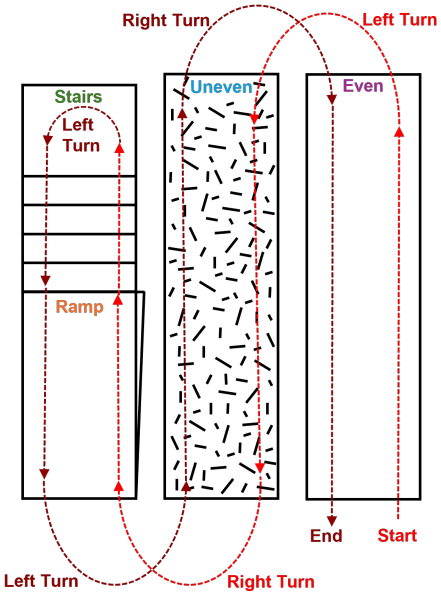

Fig. 1. Walking track containing different types of terrains (7.3m long).

sampled at 33 Hz. A custom GUI built in Python (version 3.8.1, Python Software Foundation, Wilmington, DE) and ran on a desktop computer with an Intel Core i7 CPU and 32 GB of RAM. The GUI controlled the hardware and data collection and data were saved for subsequent offline analysis.

B. Data Collection Experimental Protocol

To evaluate our framework on a dataset reflecting the complexity of real-world walking, participants navigated a mixed-terrain track at a self-selected pace. The mixed-terrain track consisted of even ground, uneven ground, up and down ramps, upstairs, downstairs, and left and right turns (Fig. 1). Each participant completed seven trials: four mixed-terrain trials traversing all types of terrain arranged in the track and three terrain-specific trials on stairs, ramps, and uneven ground to increase the number of steps for each of these terrains. Transitions between types of terrain were manually marked. A mixed-terrain dataset was constructed from all participant data. Manually marked terrain transitions were used to generate five datasets per participant: two datasets combining even ground, turns, and uneven ground; one combining even and uneven ground; one combining even ground and stairs; and one combining even ground and ramps. Of the 20 datasets (five datasets from each of the four participants), two were excluded from analysis due to technical issues, leaving 18 datasets for testing the manual and automatic parsing methods. Pressure values from each insole were normalized to the participant's weight and the area of the individual sensor cell.

C. Establishing the Ground Truth of Gait Cycle Parsing

Underfoot pressure data were upsampled by a factor of 60 from 33 Hz to 1980 Hz to increase the resolution for selecting the onset of limb loading and smoothed using a Savitzky-Golay filter (3rd order, window size = 93, derivative order = 1, rate = 1). This onset of limb loading is an inflection point in the pressure data and defined as the lowest point before a sharp positive increase in slope due to initial ground contact at the transition from swing to stance phase. Pressure profiles from each dataset were visualized for manual marking of the inflection points using a custom GUI (Python, PyQT5 library). At typical walking speeds, each gait cycle is approximately 60% stance phase and 40% swing phase [11]–[13]. The stance phase is characterized by a single or double peak, whereas during swing phase, the underfoot pressure is zero. Gait cycles with noisy or incomplete steps from shuffling, sharp turns, or tripping were excluded if they visually lacked: distinct single or double peaks, a roughly 60/40 stance-to-swing ratios, and/or near-zero pressure values during swing. All 18 datasets were manually marked, based on the above rules, by an individual with 3+ years of experience with underfoot pressure data. The experienced individual's work was validated by a gait researcher with over 6 years of experience analyzing underfoot pressure data. These cross-checked inflection points served as the ground truth for gait cycle parsing. The total number of complete gait cycles was 577.

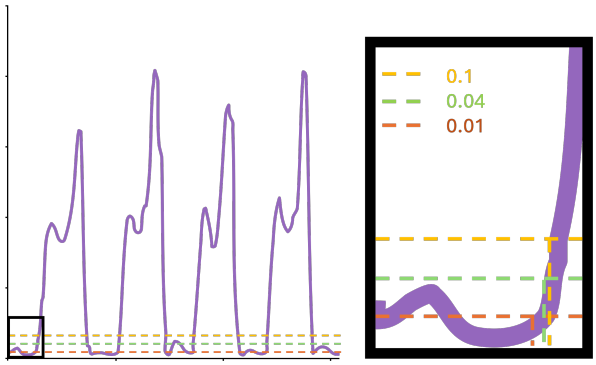

Fig. 2. Three different thresholds were applied to remove low-level noise between gait cycles. Higher thresholds removed more noise but also truncated the signal, affecting the accuracy of loading onset detection.

D. Naïve Manual Gait Cycle Parsing

To simulate naïve junior researchers manually parsing gait data, three independent researchers with no prior experience in gait analysis were recruited. Each naïve parser received instructions for using the GUI, the three criteria defining a complete gait cycle, and a reference of marked inflection points on a set of 10 gait cycles. Each researcher independently marked the same 18 datasets using the GUI. All marked points were saved in a Python dictionary and categorized by dataset for later analysis.

E. Thresholding Algorithm

Thresholding is a widely used automated method for identifying inflection points in gait data [4]. Thresholds are typically set as a multiple of the standard deviation of the background (noise) signal, or manually selected by leveraging knowledge of the particular data, making this method subjective. Thresholding often results in false positives and

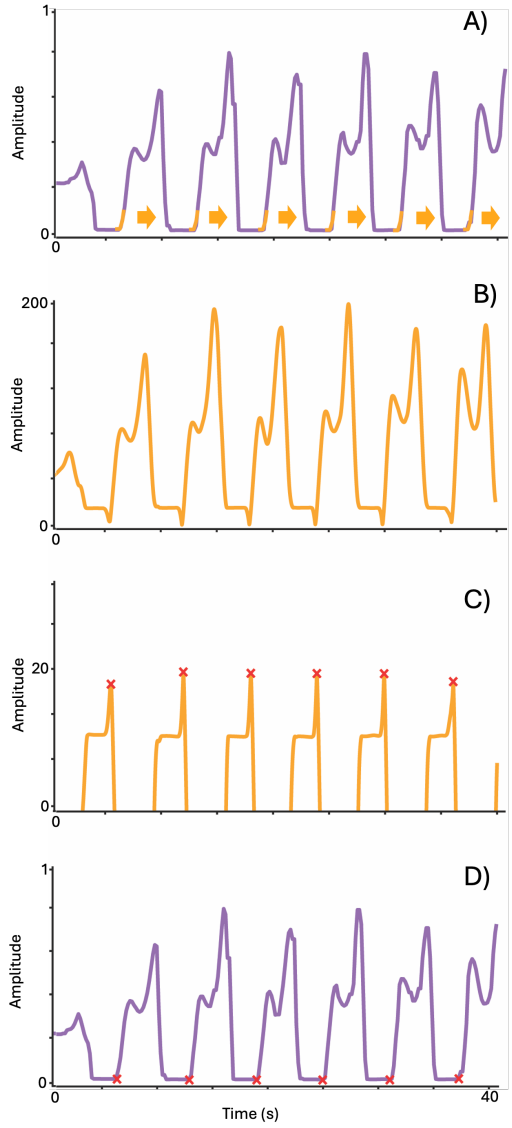

Fig. 3. Template matching algorithm flow chart. A) Iterating the template across the underfoot pressure signal to obtain the sum of the absolute difference between the raw signals and the template. B) The result of the sum of the absolute difference between the raw signals and the template. The sharp troughs indicate the point where the template best overlaps with the raw signal at the inflection point. C) Reflected signal from B about the horizontal axis, isolating the region near the peak overlap between the raw signal and the template, for each step. The peak represents the timepoint of maximum overlap (i.e., the inflection point) and is marked by a red X. D) Found inflection points mapped back onto the underfoot pressure signal, indicated by a red X.

inaccurate marking of the time of loading onset. To evaluate these limitations on parsing gait cycles, three different thresholds were tested. As gait data were normalized between 0 and 1, a low threshold of 0.01, a medium threshold of 0.04, and a high threshold of 0.1 [4] were used (Fig. 2). For each of the three thresholds, underfoot pressure values below the thresholds were set to zero, and time points where transitions from 0 to a value greater than zero were marked as inflection points. No additional programming statements were added to remove false positives or adjust positioning of the marked inflection points.

F. Template-Matching Algorithm

A total of 577 manually marked inflection points from ground truth parsing were grouped into their respective datasets (18 total). For each marked inflection point, a 200-point array was created by extracting 100 points before (including the inflection point) and 100 points after from the underfoot pressure data. These 200-point arrays were averaged within each dataset to generate a template representing the inflection point for that dataset. The final template was created by taking the average of all template arrays across all 18 datasets. The template was matched to the underfoot pressure signal by iterating the 200-point window across the signal (Fig. 3A). At each window position, the similarity between the template and the signal was quantified using the sum of absolute differences (Equation 1), producing a waveform of these differences (Fig. 3B).

$$\sum |(200 \text{ points underfoot pressure}) - \text{template}| \quad (1)$$

Regions where the template best matched the signal appeared as pronounced troughs in the difference waveform, corresponding to the points of minimum difference (Fig. 3B). To identify these troughs, the difference signal was inverted and shifted upward by 10% of its maximum value (Fig. 3C). This transformation ensured that regions far from an inflection point remained below zero. As the transformed signal rose above zero, values were stored in a buffer until it returned below zero. The index of the maximum value within each buffer was identified as the location of the template match. Identified maxima were then mapped back onto the underfoot pressure signal to mark the inflection points (Fig. 3D). Access the full open-source pipeline on GitHub [14].

G. Template-Matching Algorithm Using Subsets of the Ground Truth Inflection Points

Given the impracticality of manually parsing all inflection points, we investigated whether fewer inflection points could still yield reliable template-based parsing. Templates using 50% (282) and 25% (112) of the total ground truth inflection points were created. A 10-fold validation was performed by randomly selecting a subset of inflections points from the full dataset, building a template from these subsets, and evaluating that template's performance relative to the 100% template for each of the 10 iterations.

H. Comparing Performance of the Template-Matching Algorithm, Thresholding, and Naïve Manual Parsers

The performance of the template-matching algorithm, thresholding, and naïve researcher manual parsing were evaluated by calculating their proximity of the marked inflection points to the ground truth, as well as the number of false positives and negatives in relation to the ground truth. Comparing the location of the inflection points relative to the expert gait data (ground truth) allows for the assessment of error related to the loss of loading data at the onset and the subsequent addition of that loading data to the end of the following step. A closest-pair algorithm was used to calculate the proximity of each method's inflection points to the ground truth. The closest-pair algorithm iterated through all ground

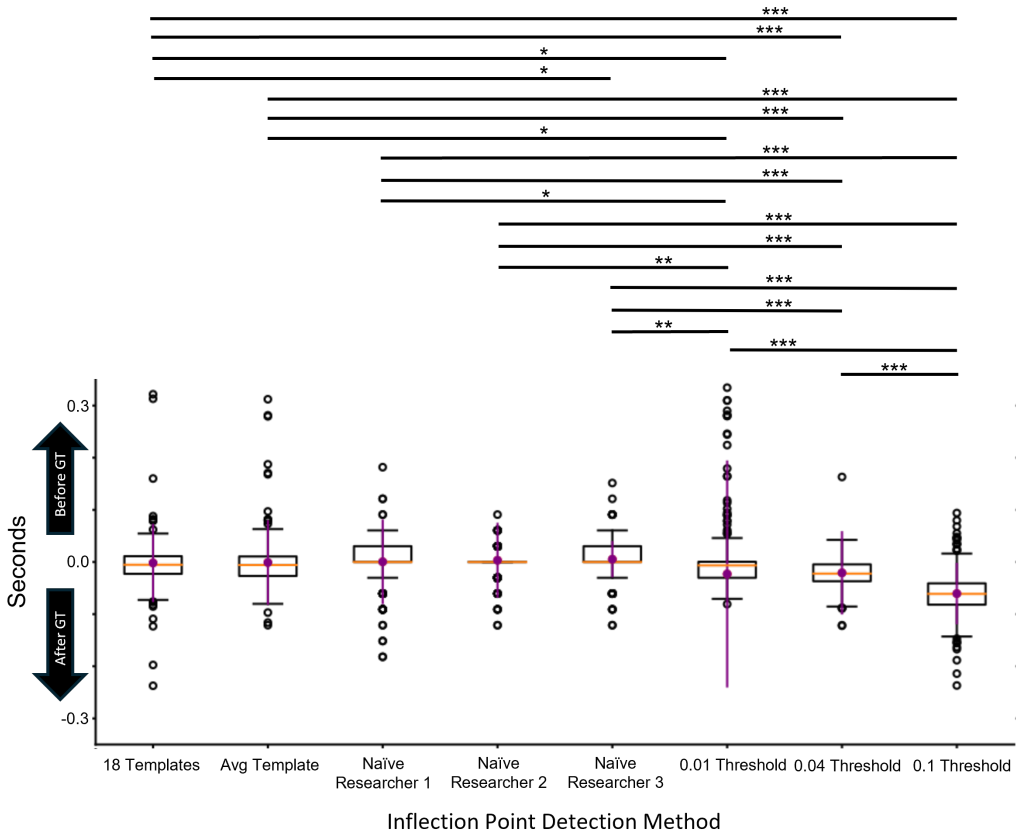

Fig. 4. Box and whisker plots of differences in inflection point location relative to the ground truth for all non-ground truth methods. Zero on the y-axis represents a perfect match with the location of the ground-truth dataset. A positive value indicates the detected inflection point occurred before the point in the ground truth. A negative value indicates the detected inflection point was after the point in the ground truth. The orange line represents the median, the box represents the first and third quartiles, and the whiskers represent the maximum and minimum for each. *p $<$ 0.05; **p $<$ 0.01; ***p $<$ 0.001.

truth inflections points, identifying the non-ground inflection point from either the template, thresholding, or naïve parsers. For each closest-pair value, the index difference between the ground truth and non-ground truth inflection point was determined. The closest-pair algorithm was also used to determine the number of false positives and false negatives of the non-ground truth methods. For example, if the naïve researcher identified 17 inflection points, and the ground truth parser identified 19, the closest pairs algorithm matched 17 points, indicating two false negatives. False positives were calculated as the total number of additional steps from the ground truth.

I. Performance of a Mean Template Built from 18 Different Templates

Building a separate template for each of the 18 datasets is not the most efficient way to parse the data. A more efficient method is to build a template that can capture the inflection points from all 18 datasets that have different cadences, step lengths, and types of terrains. To assess the performance of this mean template, all 577 inflection points were used to construct 577 templates which were then averaged to create one mean template. This mean template was then iterated across all 18 datasets identical to the methods described in section G.

J. Statistical Analysis

Normality was assessed using the Anderson-Darling test (Python's *anderson* function from the scipy.stats library). The data were nonparametric; therefore, a Kruskal-Wallis multi-group test was performed using the scipy.stats library's *kruskal* function to compare the time difference in the detection of the inflection point between all detection methods. Multiple comparisons with a Bonferroni correction were performed using Python's statsmodels.stats. *multicomp* function. The performance of the 50% and 25% templates were compared to the 100% template. For each iteration of the 10-fold validation, the Kruskal-Wallis test was performed to compare the difference in inflection point location from the ground truth for all templates. For all comparisons, a significance level less than or equal to 0.05 was considered significant.

III. Results

A. Number of Marked Inflection Points Compared to Ground Truth

Table I summarizes the total number of marked inflection points, false positives, false negatives, and the mean and standard deviation of the time between the marked inflection points and the ground truth.

TABLE I

PERFORMANCE STATISTICS FOR EACH NON-GROUND TRUTH DATASET IN RELATION TO THE GROUND TRUTH

	Marked Inflection Points #	False Positives	False Negatives	Mean Inflection Point Difference from Ground Truth (ms)	Std Inflection Point Difference from Ground Truth (ms)
18 Templates	606	28	1	-1.8	75
10x Random 50% Template	606	28	1	-1.8	73.6
10x Random 25% Template	606	28	1	0.4	76.2
Average Template	605	27	1	-1	81.2
Threshold = 0.01	939	362	0	-23	217.8
Threshold = 0.04	633	56	0	-20.8	80
Threshold = 0.1	626	49	0	-60.6	59.1
Naïve Researcher 1	544	0	33	0.4	81.3
Naïve Researcher 2	560	0	17	3.3	72
Naïve Researcher 3	571	0	6	5.3	34.5

B. Time of Marked Inflection Points Compared to Ground Truth

All methods differed significantly from the higher threshold ($p < 0.001$). The lower and medium thresholds were each different from all other methods ($p < 0.030$), except each other. Additionally, the template made of the 18 individual datasets differed from the naïve researcher 3 ($p = 0.040$). See Fig. 4. The naïve researchers marked inflection points approximately 5 ms or less before the actual onset from the ground truth (Fig. 4; Table I). For the thresholding method, all thresholds resulted in delayed detection of the inflection point, with the highest threshold resulting the largest delay (60.6 ms). The template-matching method detected the inflection point with a delay of less than 2 ms from the ground truth, accounting for less than 0.2% of a typical gait cycle duration (which is typically 1 second) [11]–[13]. The template-matching algorithm required on average 41 seconds to analyze all 18 datasets, the thresholding method required on average 22 seconds, and the manual parsers required 29 ± 2 minutes.

C. Performance of the Template-Matching Algorithm Built Using Subsets of Steps

Templates were built using a subset of steps: 50% and 25% of the total dataset containing 577 steps. The subsets of steps used for the reduced templates were randomly extracted from the full dataset 10 different times. For each 10-fold validation, the time difference of the detected inflection point between the reduced templates and the template from the full data set were compared.

The time differences ranged from -2.3 ms to 0.59 ms and -10.7 to 7.7 ms for the 50% and 25% templates, respectively. The p-values from the Kruskal-Wallis test ranged from 0.12 to 0.96, meaning that the difference in the detected time of the inflection points for the 50% template was not statistically different from the full template. However, the p-values for the 25% template ranged from 0.012 to 0.46, meaning that the time differences were sometimes statistically different.

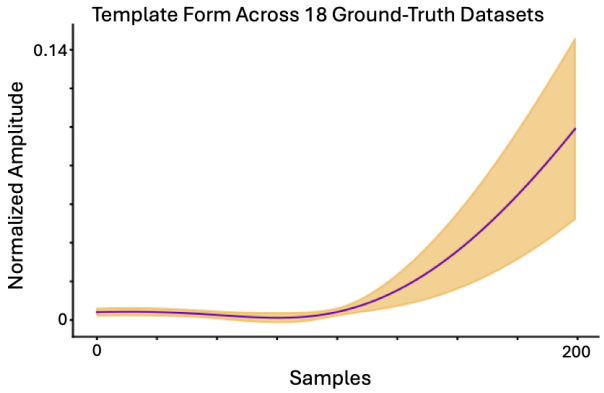

Fig. 5. Mean (± standard deviation) template shape of all templates across the 18 datasets.

IV. DISCUSSION

This work presents a novel template-matching framework that provides a low-resource, efficient, and accurate solution for gait cycle parsing across multiple terrains. Our approach is more efficient than manual parsing and more accurate than thresholding techniques, making it a practical tool for parsing large-scale gait datasets. By testing the algorithm on varying walking terrains, we demonstrated its potential for real-world applications, where traditional gait parsing methods struggle. This novel template-matching approach overcomes key limitations of existing methods and offers a transferable and accessible solution for parsing gait data in both controlled and uncontrolled settings.

Thresholding identifies the onset of loading when pressure surpasses a predefined minimum value. While computationally efficient, thresholding techniques inherently involve a trade-off between false positives and timing accuracy. This was evident in our study, as shown in Table I and Fig. 2. A lower threshold (0.01, or 1% of full scale) detected loading onset more accurately than higher thresholds (-23 ms mean difference from ground truth) but resulted in 362 false positives. In contrast, a higher threshold (0.1, or 10% of full scale) reduced false positives to 49 but introduced greater timing errors, delaying loading onset detection by -60.6 ms. This trade-off demonstrates that while increasing the threshold reduces false positives, it also shifts the detected inflection point later in the gait cycle, leading to loss of early loading pressure information. However, even at the lowest threshold, the timing of the onset of loading was significantly different compared to the template matching algorithm (Fig. 4). To mitigate false positives, researchers often implement dataset-specific catch statements to exclude misclassified steps. However, these custom rules limit generalizability across datasets which include shuffling, foot bumps, or other transient pressure fluctuations as steps. In contrast, the template-matching algorithm automatically differentiated true gait cycles from transient fluctuations, reducing false positives without custom rules.

In contrast to thresholding, which is prone to false positives, manual parsing effectively eliminates this issue but is more susceptible to false negatives. In our study, all three

naïve manual parsers exhibited fewer total errors (6–33) compared to thresholding (49–362 false positives; Table I, highlighting the relative accuracy of human annotation. The template-matching algorithm performed similarly to the naïve manual parsers, with total errors ranging from 27 to 28. Additionally, the timing of the marked inflection point, as measured by the mean difference from the ground truth in milliseconds, was statistically different between only 1 of the 3 naïve parsers when compared to the 18 template-matching algorithm and showed no statistical difference when compared to the average template algorithm (see Fig. 4). The inconsistencies among the naïve researchers highlight the limitations associated with human non-experts, which is problematic with these large-scale datasets.

The template-matching algorithm retains the strengths of manual parsing while maintaining speed (29 minutes for manual parsing compared to 41 seconds for the template-matching algorithm). With the template-matching approach, a user selects a subset of data to generate a template, which is then used to automatically identify the onset of gait cycles. This method also benefits from the low-resource nature of thresholding techniques but with improved accuracy. Additional fine-tuning of the template matching algorithm is possible using a shift parameter that enables adjustment of the height of the inverted sum absolute value signal (Fig. 3).

A limitation of the template-matching approach is the reliance on a high-quality and consistent dataset. Parsing the 577 steps with an average template constructed from all18 datasets was not significantly different in performance compared to the template made from the average of the 18 templates specific to each dataset. This demonstrates the feasibility of a generalizable template for parsing multiple datasets. There are key are some key considerations to keep in mind before using building a generalizable template. Fig. 5 displays the mean and standard deviation from the 18 different templates. There is little variability in the template values before the inflection point, and large variability in the template slope after the inflection point. Care should be taken during template construction to capture the variability in slope data after the inflection point. Cross validation, as performed here, helps to avoid biases from data sampling when constructing the template.

To further refine the template-matching algorithm, future work will involve performance testing on a larger and more diverse population, including variability in age and sex, and test its generalizability on data collected from people with gait impairments. We plan to investigate the feasibility of using the template matching algorithm for other applications and signals, specifically live or real-time parsing of data, angular velocity, reflex responses, or electrocardiography.

V. Conclusion

With this novel template-matching algorithm, large volumes of gait data can be efficiently and accurately parsed to meet the demand of modern gait analysis and rehabilitation technology development. This method successfully detected individual gait cycles from underfoot pressure data collected from participants walking across varying types of terrain. This will enable researchers to expand their gait analysis capabilities to a larger scale and beyond highly controlled laboratory settings to more variable real-world settings.

References

[1] S. D. Uhlrich, A. Falisse, Kidziński, J. Muccini, M. Ko, A. S. Chaudhari, J. L. Hicks, and S. L. Delp, "OpenCap: Human movement dynamics from smartphone videos," *PLOS Computational Biology*, vol. 19, no. 10, p. e1011462, Oct. 2023, publisher: Public Library of Science. [Online]. Available: https://shorturl.at/Gsak1

[2] A. Torres-Pardo, D. Pinto-Fernández, M. Garabini, F. Angelini, D. Rodriguez-Cianca, S. Massardi, J. Tornero, J. C. Moreno, and D. Torricelli, "Legged locomotion over irregular terrains: state of the art of human and robot performance," *Bioinspiration & Biomimetics*, vol. 17, no. 6, p. 061002, Oct. 2022, publisher: IOP Publishing. [Online]. Available: https://dx.doi.org/10.1088/1748-3190/ac92b3

[3] K. North, G. Simpson, W. Geiger, A. Cizik, D. Rothberg, and R. Hitchcock, "Predicting the Healing of Lower Extremity Fractures Using Wearable Ground Reaction Force Sensors and Machine Learning," *Sensors*, vol. 24, no. 16, p. 5321, Jan. 2024, number: 16 Publisher: Multidisciplinary Digital Publishing Institute. [Online]. Available: https://www.mdpi.com/1424-8220/24/16/5321

[4] V. N. Bobić, M. D. Djurić-Jovièić, S. M. Radovanović, N. T. Dragaević, V. S. Kostić, and M. B. Popović, "Challenges of Stride Segmentation and Their Implementation for Impaired Gait," in *2018 40th Annual International Conference of the IEEE Engineering in Medicine and Biology Society (EMBC)*, Jul. 2018, pp. 2284–2287, iSSN: 1558-4615. [Online]. Available: https://ieeexplore.ieee.org/abstract/document/8512836

[5] Y. Moon, J. Sung, R. An, M. E. Hernandez, and J. J. Sosnoff, "Gait variability in people with neurological disorders: A systematic review and meta-analysis," *Human Movement Science*, vol. 47, pp. 197–208, Jun. 2016. [Online]. Available: https://www.sciencedirect.com/science/article/pii/S0167945716300306

[6] K. North, G. M. Simpson, A. R. Stuart, E. N. Kubiak, T. J. Petelenz, R. W. Hitchcock, D. L. Rothberg, and A. M. Cizik, "Early postoperative step count and walking time have greater impact on lower limb fracture outcomes than load-bearing metrics," *Injury*, vol. 54, no. 7, p. 110756, Jul. 2023. [Online]. Available: https://www.sciencedirect.com/science/article/pii/S0020138323003881

[7] Z. Zhang, Z. Wang, H. Lei, and W. Gu, "Gait phase recognition of lower limb exoskeleton system based on the integrated network model," *Biomedical Signal Processing and Control*, vol. 76, p. 103693, Jul. 2022. [Online]. Available: https://www.sciencedirect.com/science/article/pii/S1746809422002154

[8] A. N. Dalrymple, D. A. Roszko, R. S. Sutton, and V. K. Mushahwar, "Pavlovian control of intraspinal microstimulation to produce over-ground walking," *Journal of Neural Engineering*, vol. 17, no. 3, p. 036002, May 2020, publisher: IOP Publishing. [Online]. Available: https://dx.doi.org/10.1088/1741-2552/ab8e8e

[9] A. N. Dalrymple, D. G. Everaert, D. S. Hu, and V. K. Mushahwar, "A speed-adaptive intraspinal microstimulation controller to restore weight-bearing stepping in a spinal cord hemisection model," *Journal of Neural Engineering*, vol. 15, no. 5, p. 056023, Aug. 2018, publisher: IOP Publishing. [Online]. Available: https://shorturl.at/16mZy

[10] "Gait Cycle - an overview | ScienceDirect Topics." [Online]. Available: https://www.sciencedirect.com/topics/engineering/gait-cycle

[11] "Gait Analysis: Normal and Pathological Function," *Journal of Sports Science & Medicine*, vol. 9, no. 2, p. 353, Jun. 2010. [Online]. Available: https://www.ncbi.nlm.nih.gov/pmc/articles/PMC3761742/

[12] Y. Liu, K. Lu, S. Yan, M. Sun, D. K. Lester, and K. Zhang, "Gait phase varies over velocities," *Gait & Posture*, vol. 39, no. 2, pp. 756–760, Feb. 2014. [Online]. Available: https://www.sciencedirect.com/science/article/pii/S0966636213006437

[13] F. Hebenstreit, A. Leibold, S. Krinner, G. Welsch, M. Lochmann, and B. M. Eskofier, "Effect of walking speed on gait sub phase durations," *Human Movement Science*, vol. 43, pp. 118–124, Oct. 2015. [Online]. Available: https://www.sciencedirect.com/science/article/pii/S0167945715300117

[14] "Garangatang/Gait_cycle_template_matching." [Online]. Available: https://github.com/Garangatang/Gait$_{C}ycle_{T}emplate_{M}atching$